Probing Gallate-Mediated Selectivity and High-Affinity Binding of Epigallocatechin Gallate: a Way-Forward in the Design of Selective Inhibitors for Anti-apoptotic Bcl-2 Proteins

Article *in* Applied Biochemistry and Biotechnology · March 2019

DOI: 10.1007/s12010-018-2863-7

CITATIONS
21

READS
157

5 authors, including:

Fisayo Andrew Olotu
University of KwaZulu-Natal
87 PUBLICATIONS **476** CITATIONS
SEE PROFILE

Clement Agoni
University College Dublin
65 PUBLICATIONS **350** CITATIONS
SEE PROFILE

Emmanuel Adeniji
University of KwaZulu-Natal
8 PUBLICATIONS **68** CITATIONS
SEE PROFILE

Mahmoud Soliman
University of KwaZulu-Natal
302 PUBLICATIONS **4,054** CITATIONS
SEE PROFILE

Applied Biochemistry and Biotechnology
https://doi.org/10.1007/s12010-018-2863-7

Probing Gallate-Mediated Selectivity and High-Affinity Binding of Epigallocatechin Gallate: a Way-Forward in the Design of Selective Inhibitors for Anti-apoptotic Bcl-2 Proteins

Fisayo A. Olotu[1] · Clement Agoni[1] · Emmanuel Adeniji[1] · Maryam Abdullahi[1] · Mahmoud E. Soliman[1]

Received: 14 June 2018 / Accepted: 13 August 2018/Published online: 29 August 2018

Abstract

Selective inhibition is a key focus in the design of chemotherapeutic compounds that can abrogate the oncogenic activities of anti-apoptotic Bcl-2 proteins. Although recent efforts have led to the development of highly selective BH3 mimetics, setbacks such as toxicities have limited their use in cancer therapy. Epigallocatechingallate (EGCG) has been widely reported to selectively inhibit Bcl-2 and Bcl-xL compared to other green tea phenols due to its gallate group. Herein, we investigate the interaction dynamics of EGCG at the hydrophobic grooves of Bcl-2 and Bcl-xL and the consequential effects on their BH4 domains. Arg143 and Asp108 (Bcl-2), and Glu96 and Tyr195 (Bcl-xL) formed high-affinity hydrogen interactions with the gallate group while non-gallate groups of EGCG formed weak interactions. EGCG-bound proteins showed systemic perturbations of BH4 domains coupled with the burial of crucial surface-exposed residues such as Lys17 (Bcl-2) and Asp11 (Bcl-xL); hence, a distortion of non-canonical domain interactions. Interactions of gallate group of EGCG with key hydrophobic groove residues underlie EGCG selectivity while concurrent BH4 domain perturbations potentiate EGCG inhibitory activities. Findings will aid the optimization and design of selective inhibitors that could suppress anti-apoptotic activities of Bcl2-family proteins with minimal toxicities.

Keywords EGCG · Gallate group · Anti-apoptotic · Bcl-2 · Bcl-xL · Selectivity · BH4 domain

✉ Mahmoud E. Soliman
soliman@ukzn.ac.za

[1] Molecular Bio-computation and Drug Design Laboratory, School of Health Sciences, University of KwaZulu-Natal, Westville Campus, Durban 4001, South Africa

Introduction

The ability of malignant cells to resist apoptosis presents a major factor that accounts for therapeutic failure and disease recurrence since most anticancer therapies (radio- and chemotherapies) induce malignant cell death via the apoptotic pathway [1–3]. Although several mechanisms are involved in apoptotic evasion, members of the B cell lymphoma 2 (Bcl-2) protein family play central roles in the regulation of pro- and anti-apoptotic intracellular signals [3–5]. This group of proteins contains up to four conserved Bcl-2 homology (BH) domains and is classified based on their respective involvements in the intrinsic apoptotic pathway [6]. Regulation of the apoptotic pathway involves the antagonistic effects of multidomain (BH1-4) anti-apoptotic Bcl-2 proteins on their pro-apoptotic counterparts, which are further subdivided into pro-apoptotic initiators (BH3-only) and pro-apoptotic effectors (BH1-3) [3, 6]. 3D structures of anti-apoptotic Bcl-2 proteins reveal the presence of hydrophobic grooves on their respective surfaces (formed by the BH1, BH2 and BH3 domains), which serve as binding sites for pro-apoptotic (BH3-only) proteins [3]. As previously reported, binding occurs at the hydrophobic (P2 and P4) pockets, mediated by complementary interactions with hydrophobic residues present in the BH3 motifs of BH3-only proteins [7, 8]. Anti-apoptotic proteins such as Bcl-2, Bcl-xL, and Mcl-1 sequester apoptosis effectors such as Bcl-2 antagonistic killer 1 (BAK) and Bcl-2-associated X protein (BAX) at their BH3 motifs and inhibit their activities. This describes the canonical roles of pro-survival Bcl-2 proteins in inhibiting apoptosis. BH3 only proteins such as Bcl-2-interacting mediator of cell death (BIM) and BH3-interacting domain death agonist (BID) promote apoptotic signals by downregulating anti-apoptotic Bcl-2 proteins at the mitochondria and endoplasmic reticulum [6, 9]. Also, they reportedly stimulate BAK and BAX via oligomerization, which results in the permeabilization of the mitochondrial outer membrane, cytochrome C release, and caspase activation, which altogether culminate in apoptosis [6] (Fig. 1). However, anti-apoptotic proteins are overexpressed in malignant cells where they are responsible for apoptotic dysregulation by overwhelming the pro-apoptotic machinery to enhance uncontrollable growth [3, 10].

The ability of these cells to evade apoptosis has been implicated in chemoresistance as identified in many cancers [3, 11, 12]. The oncogenic roles of anti-apoptotic Bcl-2 proteins when overexpressed present them as attractive targets in cancer therapy. Efforts to achieve direct inhibition of these proteins have led to the discovery of several inhibitor types, both synthetic and bio-derived [3, 13, 14]. More recently, the implementations of combinatorial drug discovery approaches [3] led to the design of selective inhibitors of anti-apoptotic Bcl-2 proteins such as Bcl-2, Bcl-xL, and Mcl-1, which are majorly implicated in apoptotic dysregulation [3, 13, 15]. These compounds specifically target anti-apoptotic Bcl-2 proteins and disrupt their interactions with pro-apoptotic proteins of the Bcl-2 family; hence, they are regarded as BH3 mimetics since they are able to mimic the binding activity of BH3-only pro-apoptotic proteins [3, 13]. Notable examples include dual (Bcl-2 and Bcl-xL) inhibitors; ABT-737 and ABT-263 (navitoclax), selective Bcl-2 inhibitor; ABT-199 (venetoclax) and selective Bcl-xL inhibitor; and A-1155463 among many others [3, 13, 15–18]. However, despite the high potency, selectivity, and specificity shown by these therapeutic compounds in several clinical studies [3, 13], their use has been associated with various setbacks as reviewed previously [3, 13–15]. Notable among these clinical setbacks is thrombocytopenia, which is majorly associated with the use of ABT-263, due to on-target toxicity to Bcl-xL-dependent platelets [13, 19, 20]. Likewise, monotherapeutic usage of ABT-199 (Venetoclax) have been associated with grade ¾ toxicities which entail neutropenia, anemia, thrombocytopenia, and

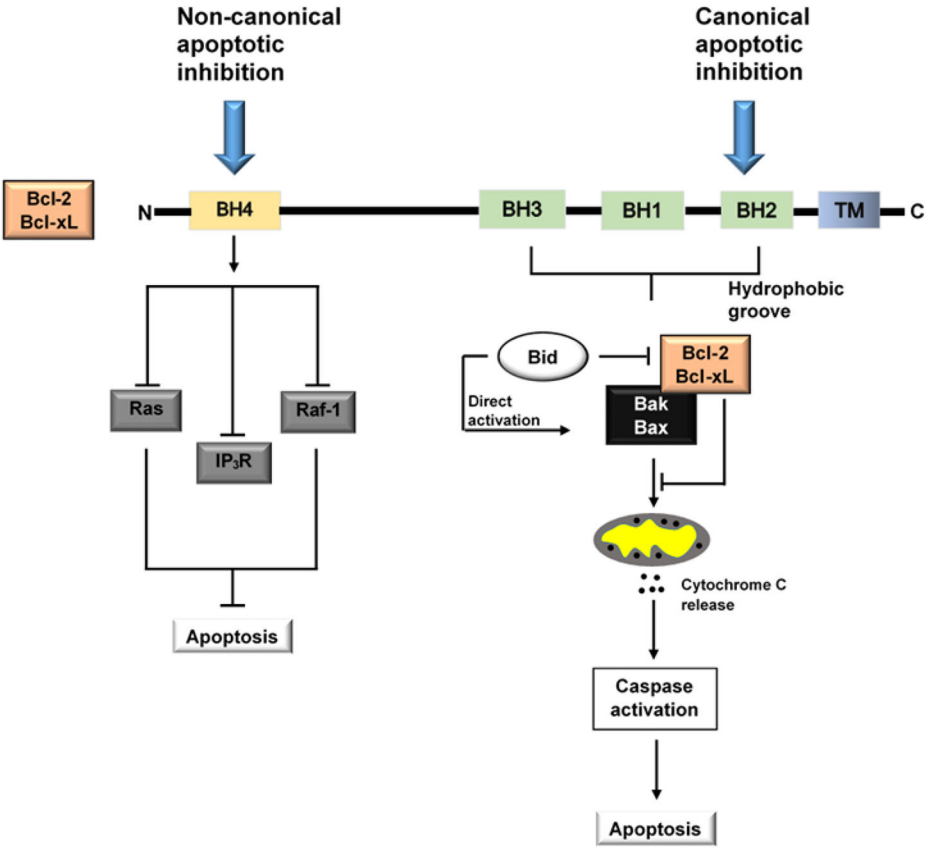

Fig. 1 Schematic representation of the canonical and non-canonical involvement of pro-survival Bcl-2 proteins in apoptotic inhibition. The BH1, BH2, and BH3 domains of anti-apoptotic Bcl-2 proteins form hydrophobic grooves with which they sequester Bak/Bax proteins and inhibit their pro-apoptotic activities, which involve permeabilization of the mitochondrial membrane, cytochrome C release, activation of executioner caspases, and eventual cell death. On the other hand, the N-terminal BH4 domain of these proteins interact with non-relatives of the Bcl-2 family to resist apoptosis

leukopenia among several others [21, 22]. On the other hand, combinatorial strategies that incorporated venetoclax and novel monoclonal antibodies (anti-CD20) have also been faced with diverse clinical setbacks, majorly due to toxic effects as previously reported [23–26]. These include neutropenia, nausea, infections, infusion reaction, and hyperkalemia, to mention but a few. Apart from toxicities, other limitations that characterize the use of BH3 mimetics include oral bio-unavailability (ABT-737) [27] and minimal sensitivity in solid tumors (ABT-199) [28, 29]. Beyond classical (canonical) anti-apoptotic roles, Bcl-2 and Bcl-xL proteins have been reported to exhibit non-canonical roles, which entail interactions with proteins that are non-relatives of the Bcl-2 family [30–32]. These interactions are attributed to their N-terminal BH4 domains, which have been implicated in certain pro-carcinogenic activities such as tumor progression, angiogenesis, and cell proliferation and migration, as previously characterized [30, 32, 33]. This domain is organized in an α-helical structure and uninvolved in the formation of the hydrophobic groove where BH3-only proteins bind, unlike the BH1, BH2, and BH3 domains (Fig. 2). In contrast, the BH4 domain is involved in many cellular functions,

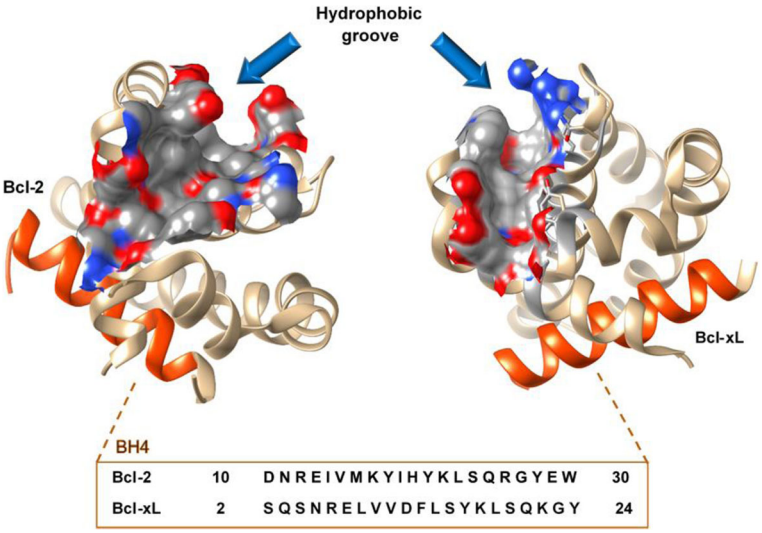

Fig. 2 Secondary structures of anti-apoptotic Bcl-2 and Bcl-xL proteins showing their respective hydrophobic grooves. The BH4 domains are colored orange while domain sequences are presented in orange inset

which makes it a superior therapeutic target [31, 33], having led to the development of molecules such as TAT-IDP^{s} (stabilized TAT-IP$_3$R-derived peptide) [34, 35] and BDA-366 [33, 36, 37] as potential BH4 domain inhibitors. The unique physiological structure and function of the Bcl-2 BH4 domain with respect to advancements made towards therapeutic targeting have been recently reviewed [30, 32, 33]. Interactions at the N-terminal BH4 domains of Bcl-2 with proteins such as rapidly accelerated fibrosarcoma (Raf-1), mitochondrial rat sarcoma (Ras), and inositol 1,4,5-triphosphate receptor (IP$_3$R) have been implicated in various mechanisms of apoptotic resistance, other than the ones elicited by the canonical binding of BH3-only proteins [33]. For instance, at the endoplasmic reticulum (ER), anti-apoptotic (Bcl-2 and Bcl-xL) proteins directly bind and inhibit the main intracellular Ca^{2+} release channel, IP$_3$R, via their N-terminal BH4 domains, thereby preventing Ca^{2+}-induced cell death, which in turn promote proliferation and apoptotic resistance [30, 33, 38, 39]. Hence, therapeutic molecules such as TAT-IDP^{s} and BDA-366, which specifically target the BH4 domains of anti-apoptotic Bcl-2 proteins, were designed to disrupt non-canonical interactions that occur in this region. Based on previous reports, TAT-IDP^{S}, a cell-permeable peptide, demonstrated the ability to disrupt the interaction between Bcl-2 and IP$_3$R, thereby enhancing calcium release from the ER which, in turn, led to apoptotic induction [33, 40, 41]. Recently, its efficacy in enhancing apoptosis has been demonstrated, not only as a single agent but also in combination with BH3 mimetics such as ABT-263 and ABT-199 [42]. On the other hand, the use BDA-366 typifies a "non-peptidic" strategy to target the BH4 domain of anti-apoptotic Bcl-2 proteins. Its efficacy has also been demonstrated in various in vivo studies and characterized by highly specific binding to BH4 domains of target proteins. According to previous studies, the interaction of BDA-366 at the BH4 domains of anti-apoptotic proteins elicit conformational changes that expose their BH3 death domains, thereby converting them into pro-apoptotic molecules [36, 43]. This underlies its (BDA-366) ability to induce apoptotic and autophagic cell death in multiple myeloma and lung cancer cell lines respectively as previously reported [37, 44]. Therefore, structural elucidation of the conformations and

dynamics of the BH4 domain with respect to therapeutic targeting of anti-apoptotic Bcl-2 and Bcl-xL proteins could provide useful insights that could enhance the structure-based design of BH4 domain inhibitors. The pro-apoptotic activities of EGCG, a green tea polyphenolic compound, have been widely explored, notably for its high-affinity binding and selectivity towards anti-apoptotic (Bcl-2 and Bcl-xL) proteins [45, 46]. These attributes have been strongly related to the presence of a gallate moiety (Fig. 3) since other green tea polyphenols lacking this group exhibited no inhibitory activity against Bcl-2 and Bcl-xL [47].

Further investigations into the selective attributes conferred on EGCG by the gallate group could be fundamental to the structure-based design of highly selective and specific inhibitors of anti-apoptotic proteins with improved therapeutic activity. In this current study, we explored the inhibitory activity of EGCG on anti-apoptotic Bcl-2 and Bcl-xL proteins, coupled with mechanistic selectivity and interactions at the surface hydrophobic groove of both proteins. Also, we investigated the structural implications of EGCG-binding on the BH4 domains of both proteins with respect to loss of domain activities. We believe that these findings will aid the development of selective inhibitors that could possibly abrogate the canonical or non-canonical anti-apoptotic activities of pro-survival Bcl-2 proteins.

Computational Methodology

System Preparation and Molecular Dynamics (MD) Simulations

X-ray crystal structures of Bcl-2 and Bcl-xL were retrieved from the Protein Data Bank with identities (PDB IDs) 4MAN and 4QVX respectively [18, 48], while EGCG was retrieved from the PubChem database (CID 65064). Using UCSF Chimera [49], co-crystallized molecules were removed from the crystal structures including crystal waters since they were observed not to be involved in the binding of ligands to the hydrophobic grooves of both proteins. Missing residues were added with the aid of MODELLER, a structural remodeling tool [50]. Molecular

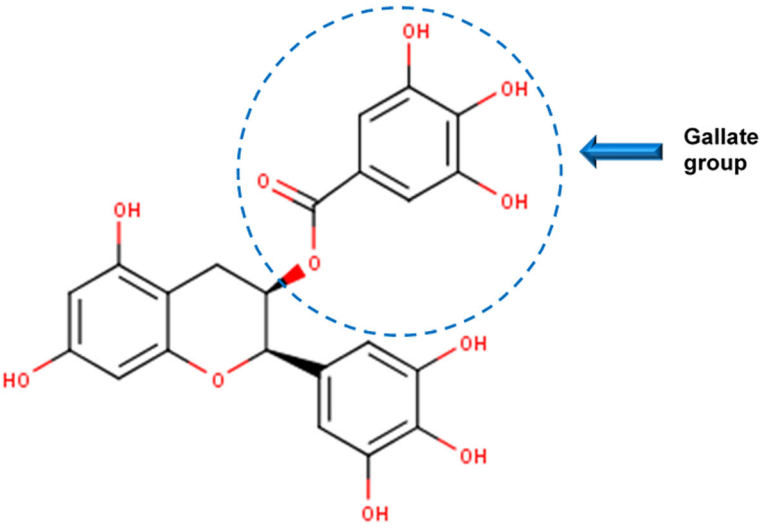

Fig. 3 Two-dimensional structure of –(-)epigallocatechingallate. Blue highlight shows the gallate group that accounts for EGCG selectivity and inhibitory activity towards Bcl-2 and Bcl-xL

geometry of the retrieved phytochemical was optimized on Avogadro 1.2.0, using a steepest descent algorithm and UFF force field [51]. This was followed by molecular docking where EGCG was docked separately into the hydrophobic grooves of Bcl2 and Bcl-xL using Autodock Vina [52]. These regions were defined according to the coordinates obtained from the crystal structures of both enzymes containing BH3 mimetics [18, 53]. The best pose with the highest negative binding energy was identified and the docked complexes were obtained using UCSF Chimera. Molecular dynamics simulations of the complexes were carried out according to the in-house protocols used in our previous studies [54–56]. These entail the use of the Graphic Processor Unit (GPU) version of AMBER14 software package coupled with integrated modules and FF14SB force field [57, 58]. The AMBER force field was used to define the protein systems while the LEAP module was used to generate parameter/topology files for the respective systems [58]. The systems were explicitly solvated in an orthorhombic TIP3P box with a size of 10 Å for all constituent atoms and counter Na^+ and Cl^- ions were added for neutralization. Partial minimization of 2500 steps was carried out with a restraint potential of 500 kcal/mol $Å^2$, followed by full minimization of 10,000 steps with no conjugate energy restraints. Harmonic restraints of 5 kcal/mol $Å^2$ were used during the heating step, which occurred gradually from 0 to 300 K for 50 ps in a canonical ensemble (NVT) with the aid of a Langevin thermostat [59]. The systems were equilibrated at a temperature of 300 K, with a 2-fs time step in an NPT ensemble for 1000 ps without any restraint while the pressure was maintained at 1 bar using the Berendsen barostat [60]. This was followed by an MD production run of 100 ns for each system, which involved the constriction of all atomic hydrogen bonds using the SHAKE algorithm [61]. Resulting coordinates and trajectories were saved every 1 ps and analyzed using the CPPTRAJ and PTRJ modules in AMBER14 [62]. Obtained data were plotted using the Microcal Origin software [63] while UCSF Chimera [49] was used for structural analysis and visualization.

Binding Free Energy Calculations

The differential binding of EGCG to Bcl-2 and Bcl-xL was estimated using the Molecular Mechanics/Poisson-Boltzmann Surface Area (MM/PBSA) method [64]. This calculates the energy involved in the complex formation and could be used to predict the strength and affinity with which small molecule compounds bind to their respective protein targets [65, 66]. Mathematically, MM/PBSA calculation is represented as follows:

$$\Delta G_{bind} = G_{complex} - G_{receptor} - G_{ligand} \quad (1)$$

$$E_{gas} = E_{int} + E_{vdw} + E_{ele} \quad (2)$$

$$G_{sol} = G_{PB} + G_{SA} \quad (3)$$

$$G_{SA} = \gamma SASA \quad (4)$$

E_{gas} shows the gas-phase energy; E_{int} is the internal energy, while E_{ele} and E_{vdw} represent the electrostatic and van der Waals interactions, respectively. The solvation free energy, denoted by G_{sol} represents the solvation free energy and can be decomposed into polar and nonpolar

contribution states. The polar solvation contribution, G_{PB}, is determined by solving the PB equation, whereas G_{SA}, the nonpolar solvation contribution, is estimated from the solvent accessible surface area (SASA) determined using a water probe radius of 1.4 Å. In addition, the crucial roles of hydrophobic groove residues to the binding, affinity, and stabilization of EGCG were investigated by estimating the per-residue energy decomposition, which revealed individual energy contributions to ligand binding.

Results and Discussion

High-Affinity Binding and Mechanistic Selectivity

According to previous studies, the gallate moiety of EGCG account for its potent inhibitory activity and selectivity towards Bcl-2 and Bcl-xL anti-apoptotic proteins since other green tea polyphenols without this moiety do not bind [47]. This suggests a possible interaction pattern that could pave way for the design of selective and potent inhibitors of these anti-apoptotic proteins. First, we measured the binding free energies of EGCG to both proteins using the MM/PBSA method. Our findings reveal favorable binding as supported by high ΔG values for both complexes (Table 1). This could indicate high-affinity binding, which agrees with its potent inhibitory activities towards Bcl-2 and Bcl-xL as previously reported [47]. It is also important to mention that the similarity in estimated energy values (Bcl-2-EGCG and Bcl-xL-EGCG) as shown in Table 1 could relatively depict analogous binding of EGCG to both proteins with respect to its selectivity and inhibitory potency. Furthermore, molecular visualization revealed hydrophobic groove interactions between constituent residues and EGCG, which accounts for its binding and stability.

Various bond types were observed between EGCG and multiple residues of the hydrophobic grooves of both proteins by reason of constituent functional groups which interacted complementarily. These include hydrogen bonds, carbon-hydrogen bonds, and aromatic interactions (Fig. 4).

Most importantly, we investigated the interaction dynamics of the gallate group at the hydrophobic grooves of both Bcl-2 and Bcl-xL along the 100-ns MD simulation time in order to identify crucial residues that "steadily" interacted with the gallate group despite its mobility and re-positioning at the hydrophobic grooves of both proteins. We believe that this approach could help unravel the mechanistic selectivity of EGCG with respect to its gallate group. At the hydrophobic groove of Bcl-2, steady hydrogen bond interactions were observed between an oxygen atom of the gallate group and side chain hydrogen atoms of Arg143 across the MD simulation time (Fig. 5).

Table 1 MMGBSA binding free energy profiles of EGCG interactions with Bcl-2 and Bcl-xL

Complexes	ΔEvdw (kcal/mol)	ΔEele (kcal/mol)	ΔGgas (kcal/mol)	ΔGsol (kcal/mol)	ΔGbind (kcal/mol)
Bcl-2-EGCG	− 35.5 ± 0.1	− 56.6 ± 0.5	− 92.0 ± 0.4	53.2 ± 0.3	− 38.8 ± 0.2
Bcl-xL-EGCG	− 36.3 ± 0.2	− 55.6 ± 0.9	− 91.9 ± 0.9	52.0 ± 0.5	− 39.9 ± 0.4

ΔEele electrostatic energy, *ΔEvdW* van der Waals energy, *ΔGbind* total binding free energy, *ΔGsol* solvation free energy, *ΔG* gas-phase free energy

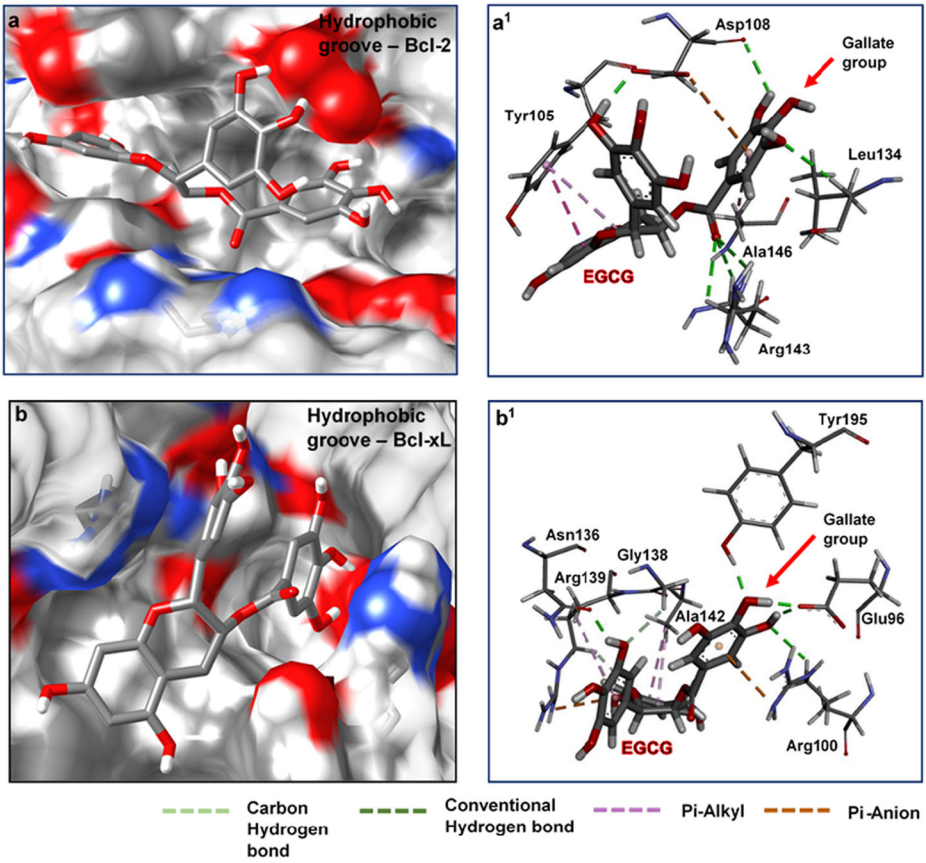

Fig. 4 Molecular visualizations of EGCG interactions at the hydrophobic grooves of (a) Bcl-2 and (b) Bcl-xL. Selective binding and inter-molecular interactions of the gallate and non-gallate EGCG groups at the hydrophobic grooves of (a^1) Bcl-2 and (b^1) Bcl-xL

These entail non-conventional (CH–O) and conventional (NH–O) hydrogen bonds with characteristic short distances ranging between 2.4 and 3.1 Å, suggestive of the crucial role of Arg143 towards the activity of the gallate group. Also, conventional (OH–O) hydrogen bond types were consistently observed along the MD simulation time, between OH groups (gallate) and oxygen atoms of Asp108, with characteristic short distances ranging between 1.5 and 2.6 Å. This could suggest that this residue is highly crucial to the activity of the gallate group. Presumably, the steady interaction of the gallate group (of EGCG) with these target residues at the hydrophobic groove underlies the mechanistic selectivity and inhibitory potency of EGCG towards Bcl-2. Likewise, at the hydrophobic groove of Bcl-xL, a similar pattern of interaction was observed between certain constituent residues and reactive atoms on the gallate group. As shown, Glu96 maintained steady (OH–O) hydrogen bond types with two OH groups present on the gallate group, with short distances ranging from 1.4 Å–1.9 Å along the 100-ns MD simulation time. This suggests the importance of Glu96 to gallate activity at the hydrophobic groove of Bcl-xL with respect to EGCG selectivity. Moreover, conventional (OH–O) and non-conventional hydrogen bond interactions (pi-donor—aromatic ring) were observed between Tyr195 and the gallate group, which could also contribute to its stability at the hydrophobic

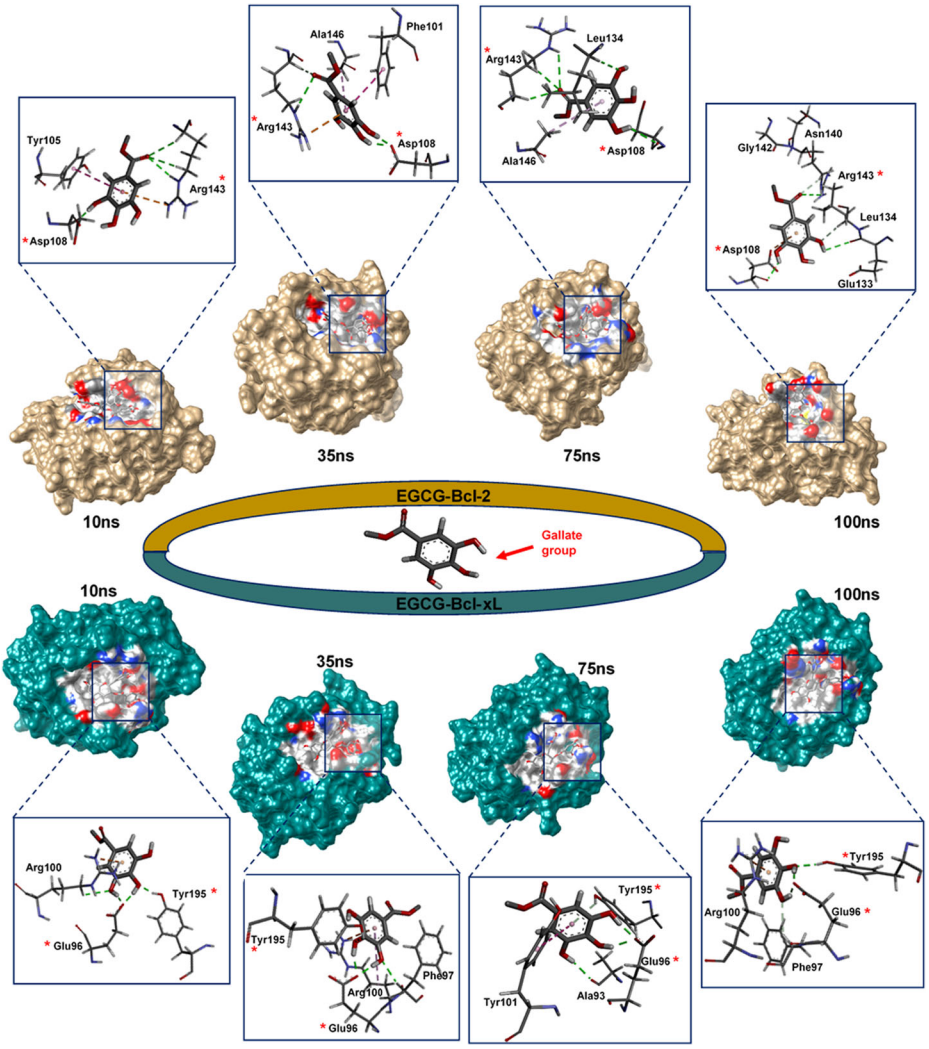

Fig. 5 Systemic binding and dynamics of the gallate group at the hydrophobic grooves of Bcl-2 and Bcl-xL, showing residues that either interacted steadily or momentarily across 100 ns MD simulation time. Residues that maintained steady interactions in both proteins are highlighted in red

groove along the MD simulation time. Taken together, this could imply that EGCG was able to selectively bind to and inhibit anti-apoptotic Bcl-2 proteins due to the specific interactions between its gallate group, Asp108 and Arg143, while in the same vein, interactions between the gallate group, Glu96 and Tyr195 account for EGCG selectively towards anti-apoptotic Bcl-xL proteins. However, quantitative analytic methods such as QM or QM/MM are more appropriate to investigate the mechanisms of bond formation between the gallate group of EGCG and these important hydrophobic groove residues, which could possibly enhance drug design and optimization techniques for novel selective inhibitors of Bcl-2 and Bcl-xL. It is also important to mention that the gallate group accounted for most of the hydrogen bonds that occurred when EGCG was bound respectively at the hydrophobic grooves of both proteins as

compared to the non-gallate groups that mostly exhibited relatively weak aromatic interactions such as pi-alkyl and pi-anion. For instance, as shown in Fig. 4(a^1) above, the gallate group exhibited five hydrogen bonds (CH–O and OH–O types) out of a total of six associated with its binding at the hydrophobic groove of Bcl-2, while in Bcl-xL, the gallate group had three hydrogen bonds (OH–O and NH–O types) out of a total of four that occurred (Fig. 4(b^1)). Moreover, these interaction patterns were observed "steadily" along the 100-ns MD simulation time as shown in Fig. 5. These findings suggest that the gallate group is basically responsible for the selectivity, high binding affinity, and inhibitory activity of EGCG and could explain the inability of other green tea polyphenols without the gallate group to bind and inhibit anti-apoptotic (Bcl-2 and Bcl-xL) proteins. This reveals the essence of the gallate moiety, most importantly for future design of highly selective and potent inhibitors of these proteins.

Per-residue energy decomposition analyses corroborated the findings above and revealed that on the average, hydrophobic residues which interacted with the gallate groups had relatively higher electrostatic energy contributions as compared to the non-gallate groups present on EGCG. In Bcl-2, energy contributions were highest in the residues that "steadily" interacted with the gallate group of EGCG; Asp108 and Arg143, with values of − 6.8 kcal/mol and − 4.2 kcal/mol respectively, indicative of their importance to the binding and stability of EGCG as earlier discussed. Other residues that "momentarily" interacted with the gallate group of EGCG at the hydrophobic groove of Bcl-2 include Ala146, Leu134, Phe101, Tyr105, Asn140, Glu133, and Gly142 with electrostatic energy contributions of − 0.2 kcal/mol, − 3.3 kcal/mol, − 1.2 kcal/mol, − 0.4 kcal/mol, − 1.6 kcal/mol, and − 0.3 kcal/mol (Fig. 6). However, it is important to mention that variations in individual energy contributions could be as a result of the different bond types occurring between interacting moieties.

Likewise, Tyr195 and Glu96 of Bcl-xL had the highest energy contributions of − 4.5 kcal/mol and − 18.5 kcal/mol. This could be related to their steady interactions with the gallate group of EGCG across the MD simulation time as shown in Fig. 5. Moreover, energy contributions for specific residues that interacted momentarily with the gallate group of EGCG along the MD simulation time include − 4.1 kcal/mol (Ala93), 1.2 kcal/mol (Arg100), − 0.5 kcal/mol (Tyr101), and − 3.7 kcal/mol (Phe97). On the other hand, energy contributions towards non-gallate groups of EGCG were mostly characterized by weak van der Waals interactions. These results further validate the importance of the EGCG gallate group, which greatly account for strong electrostatic interactions at the hydrophobic grooves of both Bcl-2 and Bcl-xL as revealed in previous analyses. Taken together, these findings could possibly enhance the structure-based design of potential "selective" inhibitors that could suppress the anti-apoptotic activities of Bcl2 and Bcl-xL more effectively.

Structural Analyses of Gallate-Mediated EGCG-Binding on the BH4 Domains

As mentioned earlier, the BH4 domains of anti-apoptotic Bcl-2 and Bcl-xL proteins have been implicated in non-canonical mechanisms of apoptotic resistance due to direct interactions with proteins that are non-members of the Bcl2 family [30, 33]. For instance, Bcl-2 pro-survival proteins have been shown to downregulate apoptosis by direct binding and inhibition of IP_3R, which in turn prevents Ca^{2+}-induced cell death, promotes proliferation, and enhances apoptotic resistance. However, while small molecule inhibitors such as BDA366 and IP_3R mimetics have been developed to curtail the inhibitory activities elicited by the BH4 domains [30], the ability of therapeutic compounds to perturb this region could also present a novel strategy to prevent pro-carcinogenic "non-canonical" roles of anti-apoptotic proteins. We propose that the

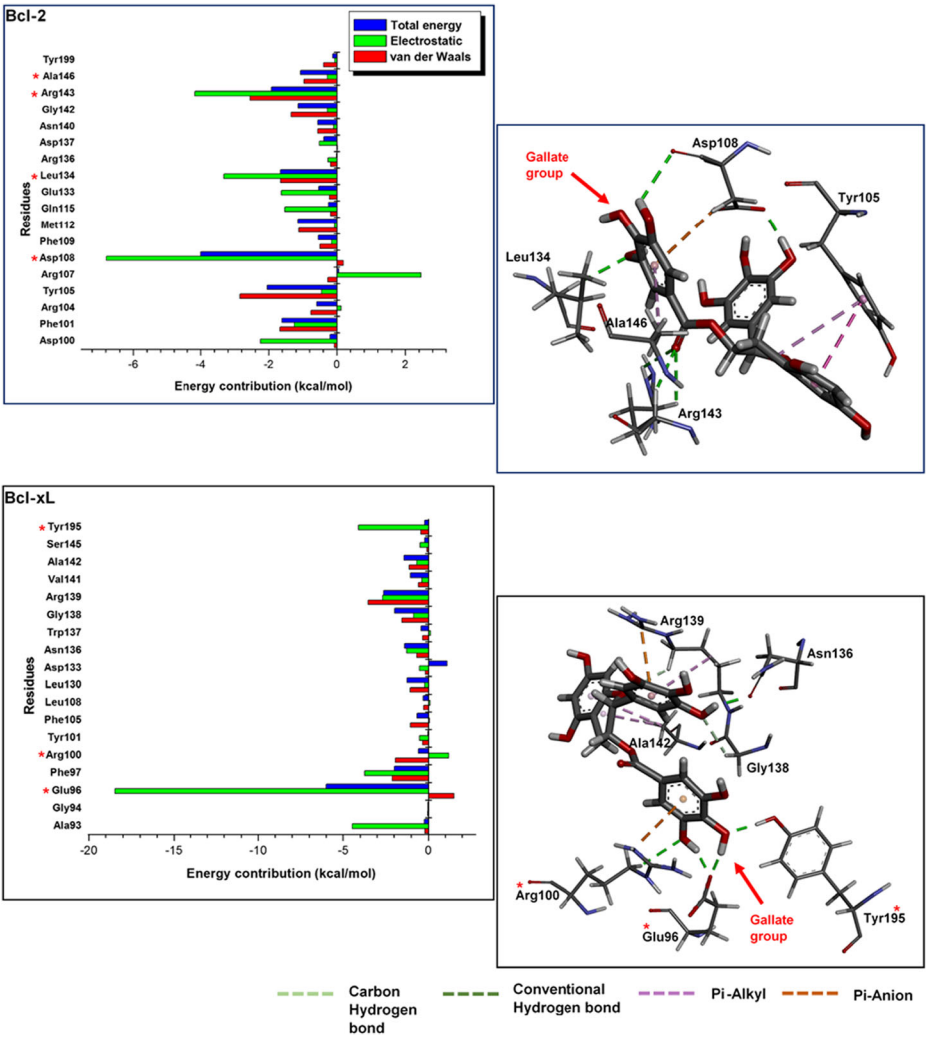

Fig. 6 Per-residue decomposition analyses showing individual energy contributions to the binding and stability of EGCG at the hydrophobic grooves of Bcl-2 and Bcl-xL. Red highlights show residues that specifically interacted with the gallate group (steadily and momentarily) and their corresponding energy contributions

high inhibitory potency associated with EGCG (gallate-mediated) could be as a result of its ability to also simultaneously perturb the BH4 domains of both Bcl-2 and Bcl-xL while binding at their surface hydrophobic grooves. This could describe its unique ability to distort the canonical and non-canonical anti-apoptotic activities of Bcl-2 and Bcl-xL proteins [30]. Therefore, we investigated the BH4 domain integrity of unbound and EGCG-bound proteins (Bcl-2 and Bcl-xL) across 100 ns MD simulation time. First, we obtained MD trajectories at intervals in order to elucidate structural occurrences across the simulation periods. These were analyzed visually using the graphical user interface (GUI) of UCSF Chimera and presented in Fig. 7. As shown, the binding of EGCG (at the hydrophobic grooves) induced systematic alterations at the BH4 domains of both proteins, indicative of structural occurrences that could possibly distort non-canonical interactions.

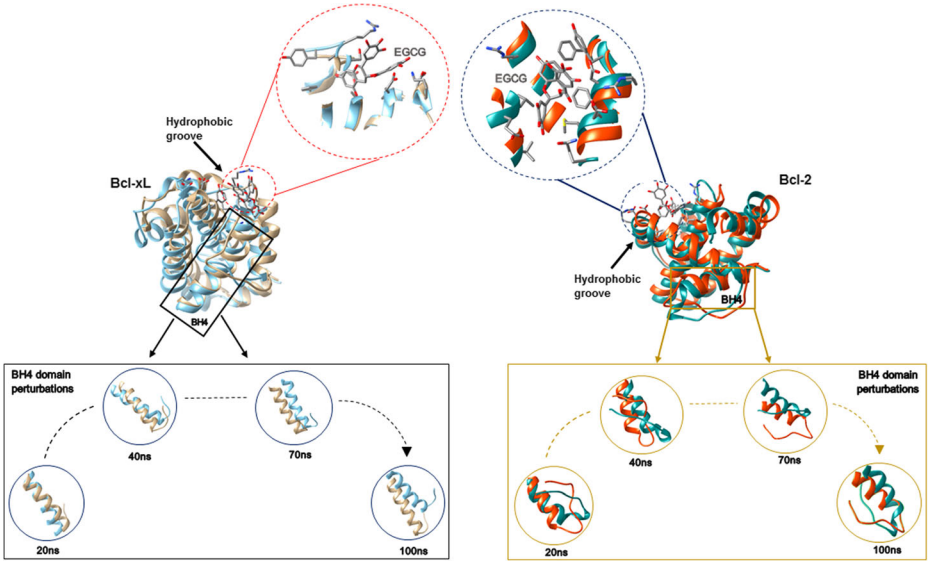

Fig. 7 Binding of EGCG at the hydrophobic grooves of Bcl-2 and Bcl-xL induce systemic perturbations at their respective BH4 domains across 100 ns MD simulation time

The degree of alterations was further measured by calculating the C-α root mean square deviation (RMSD), C-α root mean square fluctuation (RMSF), C-α radius of gyration (RoG), and solvent accessible surface area (SASA).

The C-α RMSD can be used to predict the structural stability of proteins by estimating the deviations in their backbone atoms with respect to their starting structures throughout the MD simulation time. A high RMSD value correlates with an increased structural variation and instability while a low RMSD could indicate a structurally stable protein [67]. Estimation of the RMSD revealed that the atomistic deviation was lowered in the BH4 domain of Bcl-2 and Bcl-xL when bound by EGCG as mediated by gallate group (Fig. 8a, d). Presumably, high instability characterizes active BH4 domains of Bcl-2 and Bcl-xL and could be essential for non-canonical protein-protein interactions. However, the binding of EGCG to both proteins reduce the mobility of constituent atoms, which could possibly distort non-canonical binding. Estimated mean RMSD values for unbound and EGCG-bound Bcl-2-BH4 include 3.4 Å and 2.6 Å respectively. Also, mean RMSD values for unbound and EGCG-bound Bcl-xL-BH4 include 3.0 Å and 2.5 Å respectively. C-α RMSF analyses provided further insights into the degree of fluctuations that occurred among the BH4-domain residues. This was carried out to study the effects of gallate-mediated EGCG-binding on BH4 domain plasticity with respect to the non-canonical activities since structural flexibility could indicate functionality while rigidity could imply protein inactivity [68–71]. Moreover, structural determination of the Bcl-2 family of proteins previously revealed that they exhibit domain "plasticity," which enhance their interaction and regulatory activities in the apoptotic pathway [5].

Figure 9 revealed that per-residue fluctuations at the BH4 domains were lowered in both EGCG-bound proteins as compared to the unbound forms. This could suggest that the binding of EGCG at the hydrophobic grooves of Bcl-2 and Bcl-xL concurrently lowered plasticity of their respective BH4 domains, indicative of domain inactivity. Estimated mean RMSF values for the BH4 domains of EGCG-bound Bcl-2 and Bcl-xL are 0.7 Å and 0.8 Å respectively while the unbound systems had mean values of 1.2 Å (Bcl-2) and 0.9 Å (Bcl-xL).

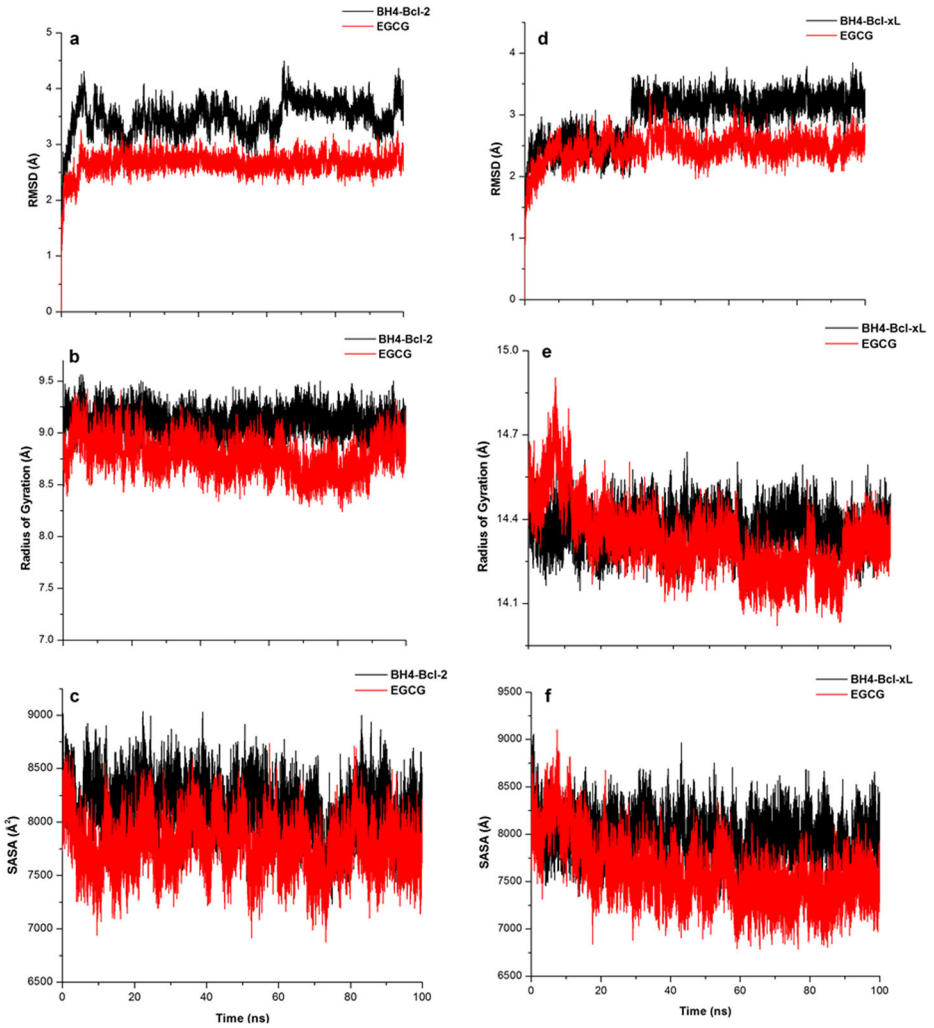

Fig. 8 **a**–**f** Combined C-α RMSD, RoG, and SASA plots showing BH4 domain alterations in unbound and EGCG-bound Bcl-2 and Bcl-xL

Furthermore, we investigated the distinct perturbations of Lys17 in Bcl-2 BH4 and Asp11 in Bcl-xL BH4, which are crucial for biological (domain) activities as previously reported [33]. Suggestively, alterations of these residues can possibly distort respective non-canonical "anti-apoptotic" activities of both proteins. Comparatively, per-residue (RMSF) calculations revealed considerable perturbations of Lys17 (Bcl-2 BH4) with mean values of 0.6 Å (unbound) and 0.5 Å (EGCG-bound). Likewise, estimated mean RMSF values for Asp11 (Bcl-xL BH4) include 0.7 Å (unbound) and 0.5 Å (EGCG-bound). Moreover, visual analysis revealed that both residues were inwardly displaced and oriented towards the hydrophobic core of the EGCG-bound proteins as compared to the unbound systems wherein they were surface-exposed (Fig. 9). Also, we determined the extent to which these residues (Lys17 and Asp11) were displaced within the unbound and EGCG-bound proteins (Bcl-2 and Bcl-xL), thereby providing additional insights into the degree of per-residue perturbations. In Bcl-2,

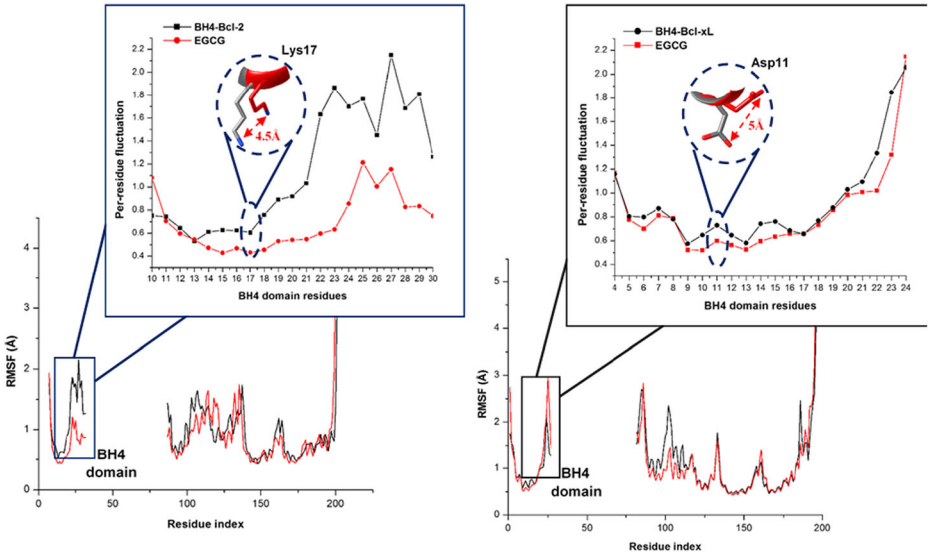

Fig. 9 Comparative C-α RMSF plots of unbound and EGCG-bound showing alterations in structural plasticity. Blue and black insets are the per-residue plots of their respective domains, which also showed inward displacement of crucial domain residues with their respective displacement distances

both the unbound and bound systems were superimposed and inter-atomic distances were measured to comparatively determine the displacement of Lys17. Likewise, this method was replicated for the unbound and EGCG-bound Bcl-xL to determine the displacement of Asp11. The results are presented in Fig. 9 and they reveal that Lys17 (BH4 Bcl-2) was displaced with a distance of 4.5 Å while Asp11 was displaced with a distance of 5.0 Å (BH4 Bcl-xL). Suggestively, perturbations of these crucial residues at the BH4 domains of both proteins could reduce the access of non-canonical binding partners, which could, in turn, distort anti-apoptotic activities. Overall alterations among BH4 domain residues were measured by calculating SASA, a parameter that depicts residue mobility and transition across the solvent (surface) and hydrophobic regions [72, 73]. This was carried out to further determine the degree of perturbations that occur at the BH4 domain when EGCG binds at the hydrophobic groove of anti-apoptotic Bcl-2 and Bcl-xL proteins. The results showed that surface-exposure of residues at the BH4 domains of both proteins were lowered across the MD simulation time (Fig. 8c, f). This agrees with the pattern of perturbations observed for Lys17 (BH4 Bcl-2) and Asp11 (BH4 Bcl-xL). Presumably, in agreement with results earlier presented, the binding of EGCG at the hydrophobic groove concurrently altered the BH4 domain by increasing the transition of "crucial" surface-exposed residues towards the hydrophobic core thereby distorting non-canonical interactions involved in apoptotic resistance. Estimated average SASA values for the BH4 domains of EGCG-bound and unbound Bcl-2 include 7773.5Å^2 and 8108.4Å^2 respectively, while average values of 7604.0Å^2 and 7937.2Å^2 were obtained for the BH4 domains of EGCG-bound and unbound Bcl-xL respectively. Additional insights into structural occurrences at the BH4 domains of both proteins were provided by estimating the C-α RoG, which was able to predict the mobility of constituent residues with respect to loss of domain activity [74]. As seen in Fig. 8b, e, residual mobility was relatively high at the BH4 domains of unbound Bcl-2 and Bcl-xL while there was a reduction in mobility at the BH4 domains of both proteins when bound by EGCG. As estimated, BH4 domains of unbound Bcl-2 and Bcl-xL had

mean RoG values of 9.2 Å and 14.5 Å respectively while EGCG-bound Bcl-2 and Bcl-xL had lower values of 8.8 Å and 14.0 Å respectively. This further agrees with results earlier presented, indicative of the possible mechanistic non-canonical inhibitory activities of EGCG towards anti-apoptotic Bcl-2 and Bcl-xL proteins, which is mediated by the gallate group. Altogether, these findings could suggest that the ability of EGCG to disrupt both canonical and non-canonical anti-apoptotic activities of Bcl-2 and Bcl-xL account for its potent inhibitory activities. These involve selective high-affinity binding at their hydrophobic grooves (canonical) and concomitant perturbations of their BH4 domains (non-canonical). In other words, while EGCG binds selectively via its gallate group at the hydrophobic grooves of both proteins, it concomitantly disrupts their respective BH4 domains, which entail systematic alterations of structural integrity and organization.

Conclusion

The ability of EGCG to selectively target and inhibit anti-apoptotic Bcl-2 proteins suggest the possibility of deriving less toxic, selective, and specific small molecule inhibitors that could complement the use of BH3 mimetics, which have been associated with toxicities. The remarkable pro-apoptotic activities of EGCG have been attributed to its constituent gallate group, and according to previous studies, other green tea polyphenols without this group are unable to bind and inhibit anti-apoptotic Bcl-2 and Bcl-xL proteins. Therefore, further investigations into the mechanistic selectivity of the EGCG gallate group at the hydrophobic groove of these proteins could help in the identification of crucial targetable residues that could possibly enhance the structure-based design of selective and potent inhibitors. In this study, we structurally elucidate the molecular basis of gallate-mediated EGCG selectivity and inhibitory potency using advanced computational techniques. Also, we investigated the possible inhibitory activity of EGCG on the non-canonical anti-apoptotic activities of these proteins by measuring concomitant perturbations at the BH4 domain. By so doing, we propose that the ability of EGCG to prevent canonical and non-canonical anti-apoptotic activities of Bcl-2 and Bcl-xL could account for its remarkable inhibitory potency, which is mediated by the presence of the gallate group. Estimations of the binding free energies revealed that EGCG exhibited favorable binding that was analogous in both proteins. Moreover, we observed that the basis of EGCG selectivity towards these proteins entails steady interactions between certain hydrophobic groove residues and the gallate group. These residues include Arg143 and Asp108 for Bcl-2, which formed conventional and non-conventional hydrogen bond types (CH–O, NH–O, OH–O), with characteristic short distances indicative of high bond strength. Likewise, the crucial roles of Glu96 and Tyr195 were identified since they exhibited similar interaction pattern with the gallate group of EGCG at the hydrophobic groove of Bcl-xL. Presumably, these residues could present a novel “suitable” target approach to achieve selective and potent inhibition of both proteins. Interestingly, we observed that the gallate group accounted for most hydrogen bond interactions that occur at the hydrophobic grooves of both proteins as compared to the non-gallate group of EGCG which were characterized with weak interactions. In the same vein, hydrophobic residues that interacted with the gallate group of EGCG (steadily or momentarily) had high electrostatic energy contributions. These findings could suggest the mode of selectivity and inhibitory potency of EGCG, which is mediated by the gallate group. Structural analyses revealed a simultaneous reduction in mobility and plasticity of Bcl-2 BH4 and Bcl-xL BH4 while EGCG was bound at their hydrophobic grooves. These

could indicate domain inactivity that could, in turn, distort non-canonical protein interactions. However, in the unbound systems, both BH4 domains were characterized by high instability and mobility indicative of domain activity. Furthermore, inward displacement and burial of crucial residues of both BH4 domains; Lys17 (Bcl-2 BH4) and Asp11 (Bcl-xL BH4) occurred while they were "surface-exposed" in the unbound protein systems where they possibly mediate non-canonical "anti-apoptotic" interactions. Moreover, these occurrences were observed for other constituent BH4-domain residues. Taken together, specific interactions between the gallate group (of EGCG) and key residues of the hydrophobic grooves (of Bcl-2 and Bcl-xL) underlie the molecular basis of EGCG selectivity while simultaneous perturbations at their respective BH4 domains potentiate EGCG inhibitory potency. Altogether, we suggest that the canonical and non-canonical inhibitory activities of EGCG are fundamental to its inhibitory potency against pro-survival Bcl-2 and Bcl-xL proteins as widely reported. We believe that these findings will aid the optimization and design of selective inhibitors that could suppress anti-apoptotic activities of Bcl2-family proteins with minimal toxicities.

Acknowledgements The authors express their profound gratitude to the College of Health Sciences, University of KwaZulu-Natal, for providing financial and infrastructural support. Also, we appreciate the Center for High Performance Computing (CHPC, www.chpc.ac.za), Capetown, South Africa, for making computational resources available.

Compliance with Ethical Standards

Conflict of Interest The authors declare that they no conflict of interest.

References

1. Baguley, B. C. (2010). Multiple drug resistance mechanisms in cancer. *Molecular Biotechnology, 46*(3), 308–316. https://doi.org/10.1007/s12033-010-9321-2.
2. Wijdeven, R. H., Pang, B., Assaraf, Y. G., & Neefjes, J. (2016). Old drugs, novel ways out: drug resistance toward cytotoxic chemotherapeutics. *Drug Resistance Updates, 28*, 65–81. https://doi.org/10.1016/j.drup.2016.07.001.
3. Ashkenazi, A., Fairbrother, W. J., Leverson, J. D., & Souers, A. J. (2017). From basic apoptosis discoveries to advanced selective BCL-2 family inhibitors. *Nature Reviews Drug Discovery., 16*(4), 273–284. https://doi.org/10.1038/nrd.2016.253.
4. Delbridge, A. R. D., Grabow, S., Strasser, A., & Vaux, D. L. (2016). Thirty years of BCL-2: translating cell death discoveries into novel cancer therapies. *Nature Reviews Cancer., 16*(2), 99–109. https://doi.org/10.1038/nrc.2015.17.
5. Kvansakul, M., & Hinds, M. G. (2015). The Bcl-2 family: structures, interactions and targets for drug discovery. *Apoptosis, 20*(2), 136–150. https://doi.org/10.1007/s10495-014-1051-7.
6. Adams, J. M., & Cory, S. (2017). The BCL-2 arbiters of apoptosis and their growing role as cancer targets. *Cell Death and Differentiation., 25*(1), 27–36. https://doi.org/10.1038/cdd.2017.161.
7. Sattler, M., Liang, H., Nettesheim, D., Meadows, R. P., Harlan, J. E., Eberstadt, M., Yoon, H. S., Shuker, S. B., Chang, B. S., Minn, A. J., Thompson, C. B., & Fesik, S. W. (1997). Structure of Bcl-x (L)-Bak peptide complex: recognition between regulators of apoptosis. *Science, 275*(5302), 983–986. https://doi.org/10.1126/science.275.5302.983.
8. Bharatham, N., Chi, S.-W., & Yoon, H. S. (2011). Molecular basis of Bcl-XL-p53 interaction: insights from molecular dynamics simulations. *PLoS One, 6*(10), e26014. https://doi.org/10.1371/journal.pone.0026014.
9. O'neill, K. L., Huang, K., Zhang, J., Chen, Y., & Luo, X. (2016). Inactivation of prosurvival Bcl-2 proteins activates Bax/Bak through the outer mitochondrial membrane. *Genes and Development, 30*(8), 973–988. https://doi.org/10.1101/gad.276725.115.

10. Zheng, J. H., Viacava Follis, A., Kriwacki, R. W., & Moldoveanu, T. (2016). Discoveries and controversies in BCL-2 protein-mediated apoptosis. *FEBS Journal., 283*(14), 2690–2700. https://doi.org/10.1111/febs.13527.
11. Gandhi, L., Camidge, D. R., De Oliveira, M. R., Bonomi, P., Gandara, D., Khaira, D., et al. (2011). Phase I study of navitoclax (ABT-263), a novel bcl-2 family inhibitor, in patients with small-cell lung cancer and other solid tumors. *Journal of Clinical Oncology, 29*(7), 909–916. https://doi.org/10.1200/JCO.2010.31.6208.
12. Vaillant, F., Merino, D., Lee, L., Breslin, K., Pal, B., Ritchie, M. E., Smyth, G. K., Christie, M., Phillipson, L. J., Burns, C. J., Mann, G. B., Visvader, J. E., & Lindeman, G. J. (2013). Targeting BCL-2 with the BH3 mimetic ABT-199 in estrogen receptor-positive breast cancer. *Cancer Cell, 24*(1), 120–129. https://doi.org/10.1016/j.ccr.2013.06.002.
13. Sarosiek, K. A., & Letai, A. (2016). Directly targeting the mitochondrial pathway of apoptosis for cancer therapy using BH3 mimetics—recent successes, current challenges and future promise. *FEBS Journal., 283*(19), 3523–3533. https://doi.org/10.1111/febs.13714.
14. Zeitlin, B. D., Zeitlin, I. J., & Nör, J. E. (2008). Expanding circle of inhibition: small-molecule inhibitors of Bcl-2 as anticancer cell and antiangiogenic agents. *Journal of Clinical Oncology., 26*(25), 4180–4188. https://doi.org/10.1200/JCO.2007.15.7693.
15. Nakajima, W., & Tanaka, N. (2016). BH3 mimetics: their action and efficacy in cancer chemotherapy. *Integrative Cancer Science and Therapeutics, 3*(3), 437–441. https://doi.org/10.15761/ICST.1000184.
16. Chen, L., & Fletcher, S. (2017). Mcl-1 inhibitors: a patent review. *Expert Opinion on Therapeutic Patents., 27*(2), 163–178. https://doi.org/10.1080/13543776.2017.1249848.
17. Beekman, A. M., & Howell, L. A. (2016). Small-molecule and peptide inhibitors of the pro-survival protein Mcl-1. *ChemMedChem, 11*(8), 802–813. https://doi.org/10.1002/cmdc.201500497.
18. Tao, Z.-F., Hasvold, L., Wang, L., Wang, X., Petros, A. M., Park, C. H., Boghaert, E. R., Catron, N. D., Chen, J., Colman, P. M., Czabotar, P. E., Deshayes, K., Fairbrother, W. J., Flygare, J. A., Hymowitz, S. G., Jin, S., Judge, R. A., Koehler, M. F. T., Kovar, P. J., Lessene, G., Mitten, M. J., Ndubaku, C. O., Nimmer, P., Purkey, H. E., Oleksijew, A., Phillips, D. C., Sleebs, B. E., Smith, B. J., Smith, M. L., Tahir, S. K., Watson, K. G., Xiao, Y., Xue, J., Zhang, H., Zobel, K., Rosenberg, S. H., Tse, C., Leverson, J. D., Elmore, S. W., & Souers, A. J. (2014). Discovery of a potent and selective BCL-XL inhibitor with in vivo activity. *ACS Medicinal Chemistry Letters, 5*(10), 1088–1093. https://doi.org/10.1021/ml5001867.
19. Rudin, C. M., Hann, C. L., Garon, E. B., Ribeiro De Oliveira, M., Bonomi, P. D., Camidge, D. R., et al. (2012). Phase II study of single-agent navitoclax (ABT-263) and biomarker correlates in patients with relapsed small cell lung cancer. *Clinical Cancer Research, 18*(11), 3163–3169. https://doi.org/10.1158/1078-0432.CCR-11-3090.
20. Mason, K. D., Carpinelli, M. R., Fletcher, J. I., Collinge, J. E., Hilton, A. A., Ellis, S., Kelly, P. N., Ekert, P. G., Metcalf, D., Roberts, A. W., Huang, D. C. S., & Kile, B. T. (2007). Programmed anuclear cell death delimits platelet life span. *Cell, 128*(6), 1173–1186. https://doi.org/10.1016/j.cell.2007.01.037.
21. Stilgenbauer, S., Eichhorst, B., Schetelig, J., Coutre, S., Seymour, J. F., Munir, T., Puvvada, S. D., Wendtner, C. M., Roberts, A. W., Jurczak, W., Mulligan, S. P., Böttcher, S., Mobasher, M., Zhu, M., Desai, M., Chyla, B., Verdugo, M., Enschede, S. H., Cerri, E., Humerickhouse, R., Gordon, G., Hallek, M., & Wierda, W. G. (2017). Venetoclax in relapsed or refractory chronic lymphocytic leukaemia with 17p deletion: a multicentre, open-label, phase 2 study. *The Lancet Oncology, 17*(6), 768–778. https://doi.org/10.1016/S1470-2045(16)30019-5.
22. Roberts, A. W., Davids, M. S., Pagel, J. M., Kahl, B. S., Puvvada, S. D., Gerecitano, J. F., Kipps, T. J., Anderson, M. A., Brown, J. R., Gressick, L., Wong, S., Dunbar, M., Zhu, M., Desai, M. B., Cerri, E., Heitner Enschede, S., Humerickhouse, R. A., Wierda, W. G., & Seymour, J. F. (2016). Targeting BCL2 with venetoclax in relapsed chronic lymphocytic leukemia. *New England Journal of Medicine, 374*(4), 311–322. https://doi.org/10.1056/NEJMoa1513257.
23. Stilgenbauer, S., Morschhauser, F., Wendtner, C.-M., Cartron, G., Hallek, M., Eichhorst, B. F., …, & Salles, G. (2016). Phase Ib study (GO28440) of venetoclax with bendamustine/rituximab or bendamustine/obinutuzumab in patients with relapsed/refractory or previously untreated chronic lymphocytic leukemia. *Blood*, *128*(22), Abstract 4393. Retrieved from http://www.bloodjournal.org/content/128/22/4393.abstract.
24. Stilgenbauer, S., Ilhan, O., Woszczyk, D., Renner, C., Mikuskova, E., Böttcher, S., et al. (2015). Safety and efficacy of obinutuzumab plus bendamustine in previously untreated patients with chronic lymphocytic leukemia: subgroup analysis of the green study. *Blood, 126*(23), 493–LP-493 Retrieved from http://www.bloodjournal.org/content/126/23/493.abstract.
25. Flinn, I. W., Gribben, J. G., Dyer, M. J. S., Wierda, W. G., Maris, M. B., Furman, R. R., et al. (2017). Safety, efficacy and MRD negativity of a combination of venetoclax and obinutuzumab in patients with previously untreated chronic lymphocytic leukemia—results from a phase 1b study (GP28331). *Blood, 130*(Suppl 1), 430–LP-430 Retrieved from http://www.bloodjournal.org/content/130/Suppl_1/430.abstract.

26. Seymour, J. F., Ma, S., Brander, D. M., Choi, M. Y., Barrientos, J., Davids, M. S., Anderson, M. A., Beaven, A. W., Rosen, S. T., Tam, C. S., Prine, B., Agarwal, S. K., Munasinghe, W., Zhu, M., Lash, L. L., Desai, M., Cerri, E., Verdugo, M., Kim, S. Y., Humerickhouse, R. A., Gordon, G. B., Kipps, T. J., & Roberts, A. W. (2017). Venetoclax plus rituximab in relapsed or refractory chronic lymphocytic leukaemia: a phase 1b study. *The Lancet Oncology, 18*(2), 230–240. https://doi.org/10.1016/S1470-2045(17)30012-8.
27. Tse, C., Shoemaker, A. R., Adickes, J., et al. (2008). ABT-263: a potent and orally bioavailable Bcl-2 family inhibitor. *Cancer Research, 68*(9), 3421–3428. https://doi.org/10.1158/0008-5472.CAN-07-5836.
28. Kelly, G. L., Grabow, S., Glaser, S. P., Fitzsimmons, L., Aubrey, B. J., Okamoto, T., Valente, L. J., Robati, M., Tai, L., Fairlie, W. D., Lee, E. F., Lindstrom, M. S., Wiman, K. G., Huang, D. C. S., Bouillet, P., Rowe, M., Rickinson, A. B., Herold, M. J., & Strasser, A. (2014). Targeting of MCL-1 kills MYC-driven mouse and human lymphomas even when they bear mutations in p53. *Genes and Development, 28*(1), 58–70. https://doi.org/10.1101/gad.232009.113.
29. Glaser, S. P., Lee, E. F., Trounson, E., Bouillet, P., Wei, A., Fairlie, W. D., Izon, D. J., Zuber, J., Rappaport, A. R., Herold, M. J., Alexander, W. S., Lowe, S. W., Robb, L., & Strasser, A. (2012). Anti-apoptotic mcl-1 is essential for the development and sustained growth of acute myeloid leukemia. *Genes and Development, 26*(2), 120–125. https://doi.org/10.1101/gad.182980.111.
30. Gabellini, C., Trisciuoglio, D., & Del Bufalo, D. (2017). Non-canonical roles of Bcl-2 and Bcl-xL proteins: relevance of BH4 domain. *Carcinogenesis, 38*(6), 579–587. https://doi.org/10.1093/carcin/bgx016.
31. Monaco, G., Vervliet, T., Akl, H., & Bultynck, G. (2013). The selective BH4-domain biology of Bcl-2-family members: IP3Rs and beyond. *Cellular and Molecular Life Sciences., 70*(7), 1171–1183. https://doi.org/10.1007/s00018-012-1118-y.
32. Akl, H., Vervloessem, T., Kiviluoto, S., Bittremieux, M., Parys, J. B., De Smedt, H., & Bultynck, G. (2014). A dual role for the anti-apoptotic Bcl-2 protein in cancer: mitochondria versus endoplasmic reticulum. *Biochimica et Biophysica Acta - Molecular Cell Research., 1843*(10), 2240–2252. https://doi.org/10.1016/j.bbamcr.2014.04.017.
33. Liu, Z., Wild, C., Ding, Y., Ye, N., Chen, H., Wold, E. A., & Zhou, J. (2016). BH4 domain of Bcl-2 as a novel target for cancer therapy. *Drug Discovery Today, 21*(6), 989–996. https://doi.org/10.1016/j.drudis.2015.11.008.
34. Akl, H., Monaco, G., La Rovere, R., Welkenhuyzen, K., Kiviluoto, S., Vervliet, T., … & Bultynck, G. (2013). IP3R2 levels dictate the apoptotic sensitivity of diffuse large B-cell lymphoma cells to an IP3R-derived peptide targeting the BH4 domain of Bcl-2. *Cell Death and Disease*, *4*(5). doi:https://doi.org/10.1038/cddis.2013.140.
35. Zhong, F., Harr, M. W., Bultynck, G., Monaco, G., Parys, J. B., De Smedt, H., et al. (2011). Induction of Ca^2+-driven apoptosis in chronic lymphocytic leukemia cells by peptide-mediated disruption of Bcl-2-IP3 receptor interaction. *Blood, 117*(10), 2924–2934. https://doi.org/10.1182/blood-2010-09-307405.
36. Han, B., Park, D., Li, R., Xie, M., Owonikoko, T. K., Zhang, G., Sica, G. L., Ding, C., Zhou, J., Magis, A. T., Chen, Z. G., Shin, D. M., Ramalingam, S. S., Khuri, F. R., Curran, W. J., & Deng, X. (2015). Small-molecule Bcl2 BH4 antagonist for lung cancer therapy. *Cancer Cell, 27*(6), 852–863. https://doi.org/10.1016/j.ccell.2015.04.010.
37. Deng, J., Park, D., Wang, M., Nooka, A., Deng, Q., Matulis, S., Kaufman, J., Lonial, S., Boise, L. H., Galipeau, J., & Deng, X. (2016). BCL2-BH4 antagonist BDA-366 suppresses human myeloma growth. *Oncotarget, 7*(19), 27753–27763. https://doi.org/10.18632/oncotarget.8513.
38. Greenberg, E. F., Lavik, A. R., & Distelhorst, C. W. (2014). Bcl-2 regulation of the inositol 1,4,5-trisphosphate receptor and calcium signaling in normal and malignant lymphocytes: potential new target for cancer treatment. *Biochimica et Biophysica Acta (BBA) - Molecular Cell Research, 1843*(10), 2205–2210. https://doi.org/10.1016/j.bbamcr.2014.03.008.
39. Chattopadhyay, P., Chaudhury, P., & Wahi, A. K. (2010). Ca+2 concentrations are key determinants of ischemia-reperfusion-induced apoptosis: significance for the molecular mechanism of Bcl-2 action. *Applied Biochemistry and Biotechnology, 160*(7), 1968–1977. https://doi.org/10.1007/s12010-009-8761-2.
40. Rong, Y.-P., Bultynck, G., Aromolaran, A. S., Zhong, F., Parys, J. B., De Smedt, H., et al. (2009). The BH4 domain of Bcl-2 inhibits ER calcium release and apoptosis by binding the regulatory and coupling domain of the IP3 receptor. *Proceedings of the National Academy of Sciences, 106*(34), 14397–14402. https://doi.org/10.1073/pnas.0907555106.
41. Rong, Y. P., Barr, P., Yee, V. C., & Distelhorst, C. W. (2009). Targeting Bcl-2 based on the interaction of its BH4 domain with the inositol 1,4,5-trisphosphate receptor. *Biochimica et Biophysica Acta - Molecular Cell Research., 1793*(6), 971–978. https://doi.org/10.1016/j.bbamcr.2008.10.015.
42. Lavik, A. R., Zhong, F., Chang, M.-J., Greenberg, E., Choudhary, Y., Smith, M. R., McColl, K. S., Pink, J., Reu, F. J., Matsuyama, S., & Distelhorst, C. W. (2015). A synthetic peptide targeting the BH4 domain of Bcl-2 induces apoptosis in multiple myeloma and follicular lymphoma cells alone or in combination with

agents targeting the BH3-binding pocket of Bcl-2. *Oncotarget, 6*(29), 27388–27402. https://doi.org/10.18632/oncotarget.4489.
43. Trisciuoglio, D., De Luca, T., Desideri, M., Passeri, D., Gabellini, C., Scarpino, S., et al. (2013). Removal of the BH4 domain from Bcl-2 protein triggers an autophagic process that impairs tumor growth. *Neoplasia, 15*(3), 315–IN37. https://doi.org/10.1593/neo.121392.
44. Deng, J., Park, D., Wang, M., Deng, Q., Matulis, S., Boise, L. H., & Deng, X. (2015). Small molecule BDA-366 as a BCL2-BH4 antagonist for multiple myeloma therapy. *Blood, 126*(23), 2049. Retrieved from http://www.embase.com/search/results?subaction=viewrecord&from=export&id=L72172345%5Cn. http://www.bloodjournal.org/content/126/23/2049.
45. Rady, I., Mohamed, H., Rady, M., Siddiqui, I. A., & Mukhtar, H. (2017). Cancer preventive and therapeutic effects of EGCG, the major polyphenol in green tea. *Egyptian Journal of Basic and Applied Sciences., 5*(1), 1–23. https://doi.org/10.1016/J.EJBAS.2017.12.001.
46. Zhao, L., Liu, S., Xu, J., Li, W., Duan, G., Wang, H., Yang, H., Yang, Z., & Zhou, R. (2017). A new molecular mechanism underlying the EGCG-mediated autophagic modulation of AFP in HepG2 cells. *Cell Death and Disease, 8*(11), e3160. https://doi.org/10.1038/cddis.2017.563.
47. Leone, M., Zhai, D., Sareth, S., Kitada, S., Reed, J. C., & Pellecchia, M. (2003). Cancer prevention by tea polyphenols is linked to their direct inhibition of antiapoptotic Bcl-2-family proteins. *Cancer Research, 63*(23), 8118–8121.
48. Souers, A. J., Leverson, J. D., Boghaert, E. R., Ackler, S. L., Catron, N. D., Chen, J., Dayton, B. D., Ding, H., Enschede, S. H., Fairbrother, W. J., Huang, D. C. S., Hymowitz, S. G., Jin, S., Khaw, S. L., Kovar, P. J., Lam, L. T., Lee, J., Maecker, H. L., Marsh, K. C., Mason, K. D., Mitten, M. J., Nimmer, P. M., Oleksijew, A., Park, C. H., Park, C. M., Phillips, D. C., Roberts, A. W., Sampath, D., Seymour, J. F., Smith, M. L., Sullivan, G. M., Tahir, S. K., Tse, C., Wendt, M. D., Xiao, Y., Xue, J. C., Zhang, H., Humerickhouse, R. A., Rosenberg, S. H., & Elmore, S. W. (2013). ABT-199, a potent and selective BCL-2 inhibitor, achieves antitumor activity while sparing platelets. *Nature Medicine, 19*(2), 202–208. https://doi.org/10.1038/nm.3048.
49. Pettersen, E. F., Goddard, T. D., Huang, C. C., Couch, G. S., Greenblatt, D. M., Meng, E. C., & Ferrin, T. E. (2004). UCSF Chimera—a visualization system for exploratory research and analysis. *Journal of Computational Chemistry, 25*(13), 1605–1612. https://doi.org/10.1002/jcc.20084.
50. Eswar, N., Webb, B., Marti-Renom, M. A., Madhusudhan, M. S., Eramian, D., Shen, M.-Y., …, & Sali, A. (2006). Comparative protein structure modeling using MODELLER. *Current protocols in bioinformatics*, *Chapter 5*, Unit-5.6. https://doi.org/10.1002/0471250953.bi0506s15.
51. Hanwell, M. D., Curtis, D. E., Lonie, D. C., Vandermeerschd, T., Zurek, E., & Hutchison, G. R. (2012). Avogadro: an advanced semantic chemical editor, visualization, and analysis platform. *Journal of Cheminformatics, 4*(8), 17. https://doi.org/10.1186/1758-2946-4-17.
52. Trott, O., & Olson, A. J. (2010). AutoDock Vina: improving the speed and accuracy of docking with a new scoring function, efficient optimization, and multithreading. *Journal of Computational Chemistry, 31*(2), 455–461. https://doi.org/10.1002/jcc.21334.
53. Leverson J, & Abbott Laboratories. (2012). ABT-199, a selective small molecule inhibitor of Bcl-2, exhibits efficacy in Bcl-2 dependent malignancies while sparing platelets. *Proceedings of AACR-NCI-EORTC Molecular Targets and Cancer Therapeutics meeting*, Abstract 036. Retrieved from http://www.ecco-org.eu/Conferences/Conferences/EORTC_NCI_AACR-2012/Searchable-program.aspx#anchorScpr.
54. Olotu, F. A., & Soliman, M. E. S. (2018). From mutational inactivation to aberrant gain-of-function: unraveling the structural basis of mutant p53 oncogenic transition. *Journal of Cellular Biochemistry, 119*(3), 2646–2652. https://doi.org/10.1002/jcb.26430.
55. Abdullahi, M., Olotu, F. A., & Soliman, M. E. (2018). Allosteric inhibition abrogates dysregulated LFA-1 activation: Structural insight into mechanisms of diminished immunologic disease. *Computational Biology and Chemistry, 73*, 49–56. https://doi.org/10.1016/j.compbiolchem.2018.02.002.
56. Ncube, N. B., Ramharack, P., & Soliman, M. E. S. (2018). An "all-in-one" pharmacophoric architecture for the discovery of potential broad-spectrum anti-flavivirus drugs. *Applied Biochemistry and Biotechnology*, pp. 1–16. https://doi.org/10.1007/s12010-017-2690-2.
57. Wang, J., Wolf, R. M., Caldwell, J. W., Kollman, P. A., & Case, D. A. (2004). Development and testing of a general AMBER force field. *Journal of Computational Chemistry, 25*(9), 1157–1174.
58. Case, D. A., Cheatham, T. E., Darden, T., Gohlke, H., Luo, R., Merz, K. M., Onufriev, A., Simmerling, C., Wang, B., & Woods, R. J. (2005). The AMBER biomolecular simulation programs. *Journal of Computational Chemistry, 26*(16), 1668–1688. https://doi.org/10.1002/jcc.20290.
59. Grest, G. S., & Kremer, K. (1986). Molecular dynamics simulation for polymers in the presence of a heat bath. *Physical Review A, 33*(5), 3628–3631. https://doi.org/10.1103/PhysRevA.33.3628.

60. Berendsen, H. J. C., Postma, J. P. M., van Gunsteren, W. F., DiNola, A., & Haak, J. R. (1984). Molecular dynamics with coupling to an external bath. *The Journal of Chemical Physics, 81*(8), 3684–3690. https://doi.org/10.1063/1.448118.
61. Ryckaert, J. P., Ciccotti, G., & Berendsen, H. J. C. (1977). Numerical integration of the cartesian equations of motion of a system with constraints: molecular dynamics of n-alkanes. *Journal of Computational Physics, 23*(3), 327–341. https://doi.org/10.1016/0021-9991(77)90098-5.
62. Roe, D. R., & Cheatham, T. E. (2013). PTRAJ and CPPTRAJ: software for processing and analysis of molecular dynamics trajectory data. *Journal of Chemical Theory and Computation, 9*(7), 3084–3095. https://doi.org/10.1021/ct400341p.
63. Seifert, E. (2014). OriginPro 9.1: scientific data analysis and graphing software—software review. *Journal of Chemical Information and Modeling, 54*(5), 1552. https://doi.org/10.1021/ci500161d.
64. Hou, T., Wang, J., Li, Y., Wang, W., Houa, T., Wangb, J., et al. (2011). Assessing the performance of the MM/PBSA and MM/GBSA methods: I. The accuracy of binding free energy calculations based on molecular dynamics simulations. *Journal of Chemical Information and Computer Sciences, 51*(1), 69–82. https://doi.org/10.1021/ci100275a.Assessing.
65. Genheden, S., & Ryde, U. (2015). The MM/PBSA and MM/GBSA methods to estimate ligand-binding affinities. *Expert Opinion on Drug Discovery, 10*(5), 449–461. https://doi.org/10.1517/17460441.2015.1032936.
66. Kalra, P., Das, A., & Jayaram, B. (2002). Free-energy analysis of enzyme-inhibitor binding: aspartic proteinase-pepstatin complexes. Applied Biochemistry and Biotechnology, 96(1–3), 93–108. Retrieved from http://eutils.ncbi.nlm.nih.gov/entrez/eutils/elink.fcgi?dbfrom=pubmed&id=11783905&retmode=ref&cmd=prlinks%5Cnfile:///_unknown_/Free-Energy Analysis of Enzyme-Inhibitor Binding - 0.pdf.
67. Bös, F., & Pleiss, J. (2009). Multiple molecular dynamics simulations of TEM beta-lactamase: dynamics and water binding of the omega-loop. *Biophysical Journal, 97*(9), 2550–2558. https://doi.org/10.1016/j.bpj.2009.08.031.
68. Mukherjee, J., & Gupta, M. N. (2015). Increasing importance of protein flexibility in designing biocatalytic processes. *Biotechnology Reports, 6*, 119–123. https://doi.org/10.1016/j.btre.2015.04.001.
69. Karshikoff, A., Nilsson, L., & Ladenstein, R. (2015). Rigidity versus flexibility: the dilemma of understanding protein thermal stability. *FEBS Journal, 282*(20), 3899–3917. https://doi.org/10.1111/febs.13343.
70. Craveur, P., Joseph, A. P., Esque, J., Narwani, T. J., & NoÃ«l, F., Shinada, N., … de Brevern, A. G. (2015). Protein flexibility in the light of structural alphabets. *Frontiers in Molecular Biosciences, 2*. https://doi.org/10.3389/fmolb.2015.00020.
71. Wallnoefer, H. G., Lingott, T., Gutiérrez, J. M., Merfort, I., & Liedl, K. R. (2010). Backbone flexibility controls the activity and specificity of a protein-protein interface: Specificity in snake venom metalloproteases. *Journal of the American Chemical Society, 132*(30), 10330–10337. https://doi.org/10.1021/ja909908y.
72. Ali, S., Hassan, M., Islam, A., & Ahmad, F. (2014). A review of methods available to estimate solvent-accessible surface areas of soluble proteins in the folded and unfolded states. *Current Protein & Peptide Science, 15*(5), 456–476. https://doi.org/10.2174/1389203715666140327114232.
73. Durham, E., Dorr, B., Woetzel, N., Staritzbichler, R., & Meiler, J. (2009). Solvent accessible surface area approximations for rapid and accurate protein structure prediction. *Journal of Molecular Modeling, 15*(9), 1093–1108. https://doi.org/10.1007/s00894-009-0454-9.
74. Lobanov, M. I., Bogatyreva, N. S., & Galzitskaia, O. V. (2008). Radius of gyration is indicator of compactness of protein structure. *Molekuliarnaia Biologiia, 42*(4), 701–706. https://doi.org/10.1134/S0026893308040195.